Drag-Induced Transfer of Horizontal Momentum between Air and Raindrops

ALAN SHAPIRO

School of Meteorology, University of Oklahoma, Norman, Oklahoma

(Manuscript received 9 January 2004, in final form 5 November 2004)

ABSTRACT

A theoretical model for unsteady drag-induced transfer of horizontal momentum between air and raindrops in moderate to heavy rainfall is presented. The model accounts for a two-way coupling in which the relative horizontal motion between air and raindrops appears as a drag forcing in both the air and raindrop equations of motion. Analytical solutions of these coupled equations are obtained for the case of rain falling through (i) an initial step change in environmental wind, (ii) a uniform shear profile, and (iii) periodically varying vertical shears of various wavenumbers (a crude proxy for turbulent eddies). Formulas for the propagation (descent) speeds of the shear zones are obtained for (ii), (iii), and for the later stage of (i). However, these speeds are generally quite small—on the order of a few centimeters per second even for heavy rainfall. More importantly, the solutions of (i) and (iii) indicate that the drag interaction leads to a decay of the velocity gradients. A formula for the *e*-folding decay time of the periodically varying shear profiles indicates that at small wavelengths, the smallest decay times are found for the smaller drops, but at large wavelengths, the smallest decay times are found for the larger drops. The decay times decrease with decreasing wavelength, and approach a value equal to the reciprocal of the product of the rainwater mixing ratio and a drag parameter in the limit of vanishing wavelength. For parameters typical of moderate to heavy rainfall, the small-scale decay times are on the order of a few minutes.

1. Introduction

By virtue of their inertia, hydrometeors falling in a turbulent or sheared environment can have substantial horizontal as well as vertical motion relative to the air. The present study is concerned with two-way drag coupling (feedback) associated with this differential motion, a subject that has received scant attention in the literature. The focus is on understanding and quantifying the role of two-way drag coupling in modifying the structure of idealized but meteorologically interesting environmental shear profiles. While the effect is found to be rather subtle, the results suggest there may be significant modification of the finescale structures (scales less than ~50 m) in moderate to heavy rainfall, or in cases of persistent rainfall.

The differential motion between hydrometeors and air (imperfect particle response) has implications for radar and aviation meteorology, where Doppler spectrum width measurements can potentially be used to detect and quantify turbulence levels (Brewster and Zrnic 1986; Meischner et al. 2001, and references therein). One of the results of the present investigation is a formula for the ratio of the amplitudes of the horizontal components of the rain and air velocities in disturbances varying periodically in the vertical (which can be thought of as periodic shear layers or as crude proxies for turbulent eddies). The formula is nearly identical to that obtained by Stackpole (1961) and Bohne (1982), even though it was derived from different physical assumptions (two-way drag coupling instead of one-way drag coupling). Thus, conclusions reached in those two previous studies concerning the interpretation of Doppler spectrum width and eddy dissipation rates in precipitation environments should also apply in the case where two-way coupling is accounted for. In particular, Bohne (1982) concluded that for radars with a 1° half-power beamwidth and 200-m pulse volume depth, failure to account for imperfect tracer response in heavy rainfall may lead to significant underestimation of turbulent intensity at short ranges (<20 km) or in regions where the outer scale of turbulence is less than 500 m. Such a scenario may well be encountered in field deployments of ground-based or airborne Doppler radars in studies of breaking Kelvin–Helmholtz waves, thunderstorm outflows, finescale structures of frontal zones,

Corresponding author address: Dr. Alan Shapiro, School of Meteorology, University of Oklahoma, 100 East Boyd, Room 1310, Norman, OK 73019.
E-mail: ashapiro@ou.edu

cumulus convection, and other small-scale convective phenomena.

The dynamical interactions associated with differential motion between air and hydrometeors are also becoming increasingly important in cloud physics studies (see review articles of Pinsky and Khain 1997; Vaillancourt and Yau 2000; Shaw 2003). For example, these interactions can lead to the preferential concentration or dispersal of particles within specific regions of the flows (e.g., through centrifuging of particles in eddies), can affect hydrometeor collection efficiencies, and may lead to rapid broadening of drop size distributions. Two-way drag coupling associated with differential particle motion may impact these processes indirectly, by reducing the amount of energy in the (small) scales affecting these processes.

Because of the complexity of the problem, most of the work on air/hydrometeor interactions has focused on one-way coupling, that is, interactions that affect the hydrometeor velocity but not the wind field. In one of the few investigations concerned with two-way coupling, Caldwell and Elliott (1972) considered the structure of the wind in a rainy surface layer. In that study, the coupled equations of motion for the air and raindrops together with a mixing length representation for the turbulent stress were solved iteratively. The resulting wind profile was found to deviate only slightly from the logarithmic wind profile, even for heavy rainfall. However, that analysis was limited to an equilibrium (steady state) flow in a shallow domain dominated by surface effects.

The present investigation is concerned with transient two-way drag coupling between air and raindrops in moderate to heavy rainfall at levels of the atmosphere high enough that surface effects can be neglected. To facilitate an understanding of this interaction and its effect on winds in the free atmosphere, a number of secondary factors are excluded from consideration. Microphysical processes such as phase changes, drop collisions, coalescence, and breakup are neglected. It is assumed that the drops are spherical, and a monodisperse drop population (equal-sized drops) is considered. The simplest possible framework is examined here, where the horizontal velocities of the air and raindrops are horizontally uniform, but are allowed to vary in the vertical and evolve in time in accord with the drag interaction. Three types of unidirectional shear structures will be analyzed: (i) initial step change in velocity profile, (ii) uniform vertical shear, and (iii) periodically varying vertical shears of various wavenumbers. Analysis of this latter flow is a preliminary step toward understanding the drag coupling in more realistic turbulent flows.

To fix the main ideas of this article, consider an environment with a step change in wind profile at some midtropospheric level $z = h$. Above this level, the wind is unidirectional with speed V, whereas beneath this level the speed is zero. At $t = 0$, rain begins to fall through the shear zone. Since the rain originates in the level above the shear zone, it initially has the same horizontal velocity component V as the air above that level. For $t > 0$, rain just falling through the shear layer exerts a lateral drag force on the initially quiescent air, inducing a lateral motion in the air. It is expected that the first raindrops to fall through the shear zone will quickly impart their lateral momentum to the air beneath the shear zone, depleting their own lateral momentum in the process, and thereafter falling through the air with negligible lateral momentum. The actual depth over which this occurs is an important parameter of the study. The drops immediately above these first drops should also impart their momentum to the air but should be able to carry their momentum downward a little further than their predecessors since the air beneath the shear zone now has nonzero horizontal momentum. In other words, the first raindrops condition the air so that the next raindrops can fall further before transferring their horizontal momentum to the air. If the rainfall is prolonged then a process where momentum is deposited at progressively lower levels is likely, resulting in a slow descent and smoothing of the shear zone.

The plan of this paper is as follows. Section 2 introduces a simple dynamical model for the two-way drag coupling between the air and raindrops and show that, for the case of unidirectional shear flow, the horizontal components of the equations of motion for the air and raindrops reduce to a single second-order linear partial differential equation. Section 3 investigates the initial value problem described above, that is, the evolution of an environment with an initial step change in wind speed. Section 4 considers the evolution of a uniform shear profile, and section 5 considers the evolution of periodically varying wind shear profiles. Section 5 also contains a simple qualitative analysis of the impact of parameterized drag on spectral energy transfer rates in a stationary energy cascade. A summary is presented in section 6.

2. Governing equations for two-way drag interaction between air and raindrops

The forces, equation of motion, and key results for a single heavy spherical particle falling through the atmosphere are described elsewhere (e.g., Stackpole 1961; Bohne 1982; Stout et al. 1993, 1995; Khain and Pinsky 1995; Pinsky and Khain 1997), and will only be briefly summarized herein. The primary forces acting on a single particle are the gravity force (corrected for buoyancy of the surrounding air) and the drag force **F** associated with relative motion between the particle and the air. Whereas the gravity force acts in the vertical, the drag force acts in the direction of the relative velocity

vector (velocity seen by an observer fixed with respect to the falling particle), and generally has three components. The drag force vector can be written as

$$\mathbf{F} = C_D \frac{\pi}{8} D^2 \rho_a V_{\rm rel} \mathbf{V}_{\rm rel}, \tag{1}$$

where C_D is the dimensionless drag coefficient, D is the particle diameter, ρ_a is the air density, $\mathbf{V}_{\rm rel} \equiv \mathbf{V}_a - \mathbf{V}_r$ is the relative velocity vector (difference between air velocity $\mathbf{V}_a$ and particle velocity $\mathbf{V}_r$), and $V_{\rm rel} \equiv |\mathbf{V}_{\rm rel}|$ is the relative particle speed. Experiments with spherical particles have shown that C_D is a function of the Reynolds number, $\mathrm{Re} \equiv \rho V_{\rm rel} D/\mu$, where μ is the dynamic viscosity of air. The functional relation $C_D = f(\mathrm{Re})$ has been determined experimentally for a large range of Re, and is well approximated by empirical formulas.

A particle falling through still air accelerates until the magnitude of the drag force (1) is large enough to balance the gravity force. The vertical velocity in this steady state is known as the terminal velocity. The behavior of a particle falling through a turbulent environment is more complex. At small values of Re (Stokes regime), C_D varies inversely with Re, so an increase in $V_{\rm rel}$ associated with a wind gust is countered by a decrease in C_D. However, at large values of Re ($10^2 < \mathrm{Re} < 10^4$), C_D is relatively insensitive to Re, and increases in $V_{\rm rel}$ are more effective at increasing the drag force. Thus, the settling velocity of a heavy particle encountering wind gusts is reduced from what it would be in a still fluid. However, as shown in Fig. 13 of Stout et al. (1995), the magnitude of this effect is small for low to moderate turbulence levels. In this study we suppose this effect is of secondary importance, and consider the vertical velocity of the drop to be little changed from its terminal velocity value in still air, a restriction also adopted by Stackpole (1961), Bohne (1982), and Khain and Pinsky (1995).

Now consider a tiny volume of air containing, at some instant of time, a mixture of dry air of mass M_a and a monodisperse population of N raindrops of diameter D, density ρ_r, and velocity $\mathbf{V}_r$. The total mass of the drops in this volume is $M_r \equiv N m_r$, where $m_r \equiv \rho_r (4/3)\pi (D/2)^3$ is the mass of an individual drop. The net drag of the dry air on the drops within the volume is $N\mathbf{F}$ where $\mathbf{F}$ is given by (1). By Newton's principle of action and reaction, the drops exert an equal and opposite force $-N\mathbf{F}$ on the dry air. Accordingly, the equation of motion for the drops can be written as

$$M_r \frac{d\mathbf{V}_r}{dt} = N\mathbf{F} + \mathbf{B}_r, \tag{2}$$

where $\mathbf{B}_r$ is the (buoyancy corrected) gravity force on the drops, and d/dt is the total derivative following the motion of the drops, while the equation of motion for the dry air can be written as

$$M_a \frac{D\mathbf{V}_a}{Dt} = -N\mathbf{F} + \mathbf{B}_a, \tag{3}$$

where $\mathbf{B}_a$ is the sum of the (vertical) pressure gradient force and the gravity force, and D/Dt is the total derivative following the motion of the air. Dividing (2) and (3) by M_r and M_a, respectively, and using (1) for $\mathbf{F}$, we obtain

$$\frac{d\mathbf{V}_r}{dt} = \left(\frac{3}{4}\frac{\rho_a}{\rho_r}\frac{C_D}{D} V_{\rm rel}\right)\mathbf{V}_{\rm rel} + \frac{\mathbf{B}_r}{M_r}, \tag{4}$$

$$\frac{D\mathbf{V}_a}{Dt} = -q_r\left(\frac{3}{4}\frac{\rho_a}{\rho_r}\frac{C_D}{D} V_{\rm rel}\right)\mathbf{V}_{\rm rel} + \frac{\mathbf{B}_a}{M_a}, \tag{5}$$

where

$$q_r \equiv M_r/M_a \tag{6}$$

is the rainwater mixing ratio.

In this study the horizontal velocity components of the air and raindrops are treated as horizontally homogeneous and unidirectional, though with magnitudes that vary in the vertical. It is also supposed that the air and raindrop vertical velocities can be approximated as constants, at least over the largest vertical dimensions considered in this study, which is on the order of 10^2 m. The type of vertical air motion envisioned (if any) is of a slow mesoscale ascent or descent at midlevels of the atmosphere, however this motion is not an important feature of the study. A Cartesian coordinate system is introduced in which one axis (say, y axis) is oriented in the direction of the wind, while the z axis points upward. The air, rain, and relative velocity vectors can then be written as $\mathbf{V}_a = \upsilon_a\mathbf{j} + w_a\mathbf{k}$, $\mathbf{V}_r = \upsilon_r\mathbf{j} + w_r\mathbf{k}$, and $\mathbf{V}_{\rm rel} = (\upsilon_a - \upsilon_r)\mathbf{j} + (w_a - w_r)\mathbf{k}$, where $\mathbf{j}$ and $\mathbf{k}$ are unit vectors pointing along the positive y and z axes, respectively, $\upsilon_a = \upsilon_a(z, t)$ and $\upsilon_r = \upsilon_r(z, t)$ are the horizontal components of the air and rain velocity, and w_a and w_r are the (constant) air and rain vertical velocity components. Taking the dot product of (4) and (5) with $\mathbf{j}$ (noting that $\mathbf{B}_r$ and $\mathbf{B}_a$ only project in the $\mathbf{k}$ direction), and expanding the total derivatives as $d/dt = \partial/\partial t + w_r\partial/\partial z$ and $D/Dt = \partial/\partial t + w_a\partial/\partial z$, we obtain

$$\frac{\partial \upsilon_r}{\partial t} + w_r\frac{\partial \upsilon_r}{\partial z} = \left(\frac{3}{4}\frac{\rho_a}{\rho_r}\frac{C_D}{D} V_{\rm rel}\right)(\upsilon_a - \upsilon_r), \tag{7}$$

$$\frac{\partial \upsilon_a}{\partial t} + w_a\frac{\partial \upsilon_a}{\partial z} = -q_r\left(\frac{3}{4}\frac{\rho_a}{\rho_r}\frac{C_D}{D} V_{\rm rel}\right)(\upsilon_a - \upsilon_r). \tag{8}$$

TABLE 1. Examples of raindrop parameters and eddy decay times (small-wavelength limit) at 700 mb.

					Eddy decay times T_e (s) for small wavelengths				
D (mm)	w_t (m s^{-1})	Re	C_D	λ (s^{-1})	$q_r = 0.001$	$q_r = 0.002$	$q_r = 0.003$	$q_r = 0.004$	$q_r = 0.005$
1.0	−4.5	240	0.71	2.18	459	229	153	115	92
1.5	−6.3	510	0.55	1.58	633	316	211	158	127
2.0	−7.7	820	0.48	1.26	794	397	265	198	159
2.5	−8.7	1160	0.44	1.05	952	476	317	238	190
3.0	−9.3	1490	0.42	0.89	1124	562	375	281	225

Attention is restricted to terminal velocities $w_t \equiv w_r - w_a$ so much larger than $v_r - v_a$ that $V_{\rm rel} = [(v_r - v_a)^2 + w_t^2]^{1/2}$ can be safely approximated as $V_{\rm rel} \sim |w_t|$ (if $v_r - v_a$ was as large as 10% of w_t, the relative error in $V_{\rm rel}$would be only ~0.5%, while if $v_r - v_a$ was as large as 30% of w_t, the relative error in $V_{\rm rel}$ would rise to only ~4.5%). Since w_a and w_r are treated as constant, w_t is also constant. The constancy of these variables is consistent with the restriction that $v_r - v_a$ contributes negligibly to $V_{\rm rel}$. If $v_r - v_a$ did become large, the drag term in the vertical component of (4) would affect the vertical velocity in the manner described above.

Since the air velocity field is horizontally homogeneous with constant vertical component, the Boussinesq form of mass conservation (incompressibility condition) is satisfied identically. These same restrictions on the raindrop velocity field and the assumed monodisperse drop size distribution ensure that the conservation law for drop concentration is also satisfied [Eq. (17) of Shaw (2003)].

In view of the constancy of w_t (and D), the Reynolds number and drag coefficient C_D are also constant, and it is convenient to introduce the (constant) drag parameter

$$\lambda \equiv \frac{3}{4}\frac{\rho_a}{\rho_r}\frac{C_D}{D}|w_t|. \tag{9}$$

Later, when the two-way coupling results are compared with results from previous one-way coupling studies, we will use the relation $\lambda = -g(1 - \rho_a/\rho_r)/w_t$, which follows from the vertical component of (4).

It is also convenient to work in a frame of reference moving vertically with the air. The space and time variables in the moving frame are

$$Z = z - w_a t - h, \quad T = t, \tag{10}$$

where h is a reference altitude which will be identified as the initial height of a shear zone. In the moving frame, the equations of motion (7) and (8) become

$$\frac{\partial v_r}{\partial T} + w_t\frac{\partial v_r}{\partial Z} = \lambda(v_a - v_r), \tag{11}$$

$$\frac{\partial v_a}{\partial T} = -q_r\lambda(v_a - v_r). \tag{12}$$

Using (12) to eliminate v_r in favor of v_a in (11) results in a second-order linear hyperbolic partial differential equation,

$$\frac{\partial^2 v_a}{\partial T^2} + w_t\frac{\partial^2 v_a}{\partial Z\partial T} + \lambda(q_r + 1)\frac{\partial v_a}{\partial T} + \lambda q_r w_t\frac{\partial v_a}{\partial Z} = 0. \tag{13}$$

3. Initial value problem: Step change in wind profile

In this section we will look at the evolution of an initial velocity discontinuity after the onset of rainfall. Suppose the initial horizontal velocity components of the rain and air jump by a factor of V at $z = h$ (i.e., $Z = 0$)

$$v_r(Z, 0) = v_a(Z) = VH(Z), \tag{14}$$

where $H(Z)$ is the Heaviside unit step function (=0 for $Z < 0$, =1 for $Z > 0$).

Since the first drops to pass through the shear zone are exposed to undisturbed air ($v_a = 0$) throughout their descent, the equation of motion (11) for these leading edge drops can be written as $dv_r/dT = -\lambda v_r$, which has the solution $v_r = V\exp(-\lambda T)$. Thus, $1/\lambda$ is the horizontal relaxation (e-folding) time scale, the time over which drops falling through an undisturbed environment reduce their horizontal momentum to $1/e$ of their initial value. For the moderate to heavy rain parameters considered in Table 1, the relaxation times are on the order of 1 s.

Integrating (11) and (12) across the lengthening column bounded on the bottom by the leading edge drops $[Z_b(T) \equiv w_t T]$ and at top by the initial height of the shear zone ($Z = 0$) [using Leibnitz rule, $dZ_b/dT = w_t$, and $v_a(Z_b) = 0$], we obtain the coupled linear ordinary differential equations,

$$\frac{d}{dT}\int_{Z_b(T)}^{0} v_r\,dZ + w_t V = \lambda\left[\int_{Z_b(T)}^{0} v_a\,dZ - \int_{Z_b(T)}^{0} v_r\,dZ\right], \tag{15}$$

$$\frac{d}{dT}\int_{Z_b(T)}^{0} v_a\,dZ = -q_r\lambda\left[\int_{Z_b(T)}^{0} v_a\,dZ - \int_{Z_b(T)}^{0} v_r\,dZ\right]. \tag{16}$$

The solution of (15) and (16) subject to $Z_b(0) = 0$ is obtained as

$$\int_{Z_b(T)}^{0} v_r\,dZ = -\frac{w_t V q_r}{1+q_r}T - \frac{w_t V}{(1+q_r)^2\lambda}[1 - e^{-(1+q_r)\lambda T}], \tag{17a}$$

$$\int_{Z_b(T)}^{0} v_a\,dZ = -\frac{w_t V q_r}{1+q_r}T + \frac{w_t V q_r}{(1+q_r)^2\lambda}[1 - e^{-(1+q_r)\lambda T}]. \tag{17b}$$

Subtracting (17b) from (17a), we obtain the integrated velocity defect as

$$\int_{Z_b(T)}^{0} (v_r - v_a)\,dZ = -\frac{w_t V}{(1+q_r)\lambda}[1 - e^{-(1+q_r)\lambda T}]. \tag{18}$$

For the usual meteorological case where $q_r \ll 1$, and for times greater than a few horizontal relaxation time scales (at most a few seconds), (17a), (17b), and (18) are well approximated by

$$\int_{Z_b(T)}^{0} v_r\,dZ \approx -\frac{w_t V}{\lambda}(\lambda q_r T + 1), \tag{19a}$$

$$\int_{Z_b(T)}^{0} v_a\,dZ \approx -\frac{w_t V q_r}{\lambda}(\lambda T - 1), \tag{19b}$$

$$\int_{Z_b(T)}^{0} (v_r - v_a)\,dZ \approx -\frac{w_t V}{\lambda}. \tag{20}$$

Thus, the column length and column-integrated velocity profiles increase linearly with time, but the column-integrated velocity defect is constant. Since $-w_t/\lambda$ is the distance a drop falls in one relaxation time, the velocity defect Eq. (20) has a simple interpretation: the area between the rain and air velocity profiles in the column at any time is equal to the corresponding area after one relaxation time [approximately the column depth $-w_t/\lambda$ times a velocity defect in which $v_r = V$ (value when drops cross shear zone) and $v_a = 0$ (undisturbed air velocity value)].

The solution of the initial value problem (13) and (14) is obtained in appendix A as

$$v_a = \begin{cases} V, & Z > 0, \\ Ve^{-\lambda Z/w_t}\displaystyle\int_0^{\lambda q_r(T - Z/w_t)} e^{-u} I_0(2\sqrt{\lambda Z u/w_t})\,du, & -T < -Z/w_t < 0, \\ 0, & -Z/w_t < -T < 0. \end{cases} \tag{21}$$

where I_0 is the modified Bessel function of the first kind of order zero [properties of modified Bessel functions are described in Abramowitz and Stegun (1964) and other standard references].

Nondimensionalizing variables as $Z^* \equiv -\lambda Z/w_t$ (Z^* and Z have same sign since $w_t < 0, \lambda > 0$), $T^* \equiv \lambda T$, and $v^* \equiv v_a/V$, (21) becomes

$$v^* = \begin{cases} 1, & Z^* > 0, \\ e^{Z^*}\displaystyle\int_0^{q_r(T^* + Z^*)} e^{-u} I_0(2\sqrt{-Z^* u})\,du, & -T^* < Z^* < 0, \\ 0, & Z^* < -T^* < 0. \end{cases} \tag{22}$$

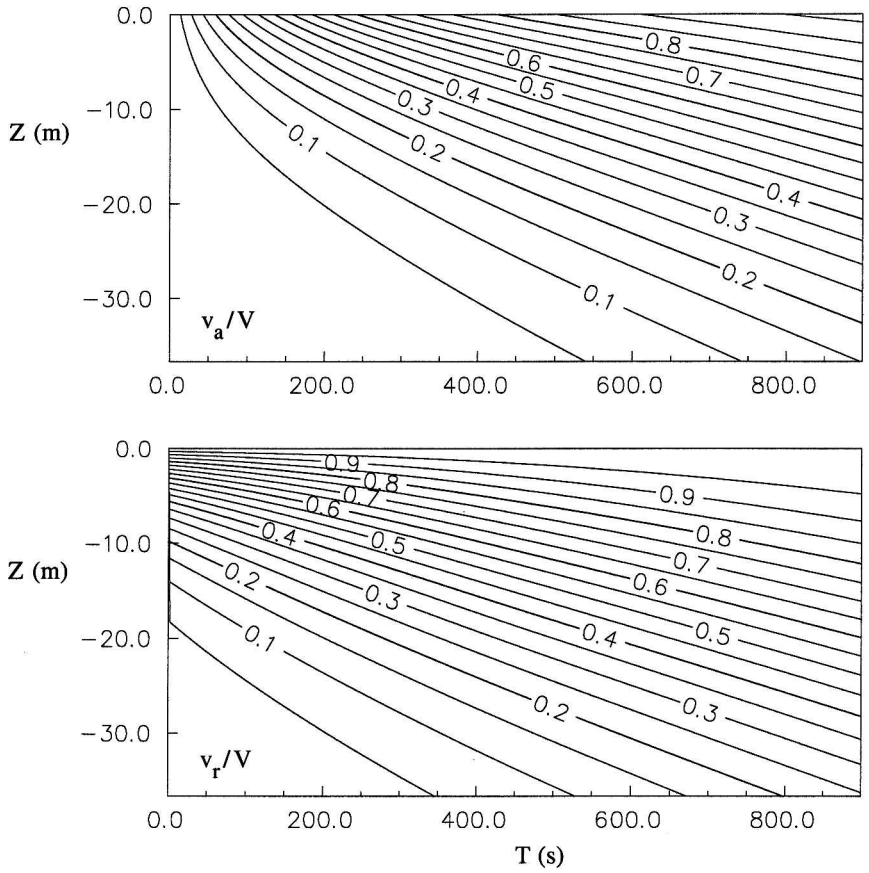

FIG. 1. Contour plots of (top) v_a/V and (bottom) v_r/V for heavy rain falling through a shear zone. Rainwater mixing ratio $q_r = 0.003$. Drop diameter $D = 2$ mm.

A simpler expression is obtained for the local derivative of v^*:

$$\frac{\partial v^*}{\partial T^*} = \begin{cases} 0, & Z^* > 0, \\ q_r e^{-q_r T^* + (1-q_r) Z^*} I_0[2\sqrt{-q_r Z^*(T^* + Z^*)}], & -T^* < Z^* < 0, \\ 0, & Z^* < -T^* < 0. \end{cases} \tag{23}$$

For the results presented herein, I_0 is evaluated with the first ten terms of its ascending series representation for arguments less than 10, and with the first four terms of its asymptotic expansion for arguments greater than 10. The integral in (22) is evaluated with the trapezoidal formula.

As an illustrative example, consider heavy rainfall with mixing ratio $q_r = 0.003$ kg rainwater per kg dry air, drop diameter $D = 0.002$ m, and drop density $\rho_r = 10^3$ kg m^{-3} falling through a shear zone at $z = 3$ km. The standard atmosphere pressure, density, and temperature at this level are $p \sim 700$ mb, $\rho_a \sim 0.91$ kg m^{-3} and $T_a \sim 268.6$ K, respectively, and the dynamic viscosity (which varies only with temperature) is $\mu \sim 1.7 \times 10^{-5}$ kg m^{-1} s^{-1} (Kundu and Cohen 2002). The terminal velocity of the drops as estimated from Fig. 7 of Beard (1976) is $w_t \sim 7.7$ m s^{-1}. The corresponding Reynolds number is Re $\sim$ 820, and the drag coefficient as estimated from (3-225) of White (1991) is $C_D \sim 0.48$ [see also Fig. 2 of Stout et al. (1995); and curve 1 of Fig. 5 of Beard (1976)]. Equation (9) then yields $\lambda \sim 1.26$ s^{-1}. These data and the parameters for a variety of moderate-to-heavy-rain scenarios are summarized in Table 1.

Contour plots of the air velocity v_a as calculated from (21) and rain velocity v_r as computed as a residual from (12) are presented in Fig. 1. Vertical profiles of these variables at two times (2 and 15 min after onset of rainfall) are shown in Fig. 2. Qualitatively, we see that

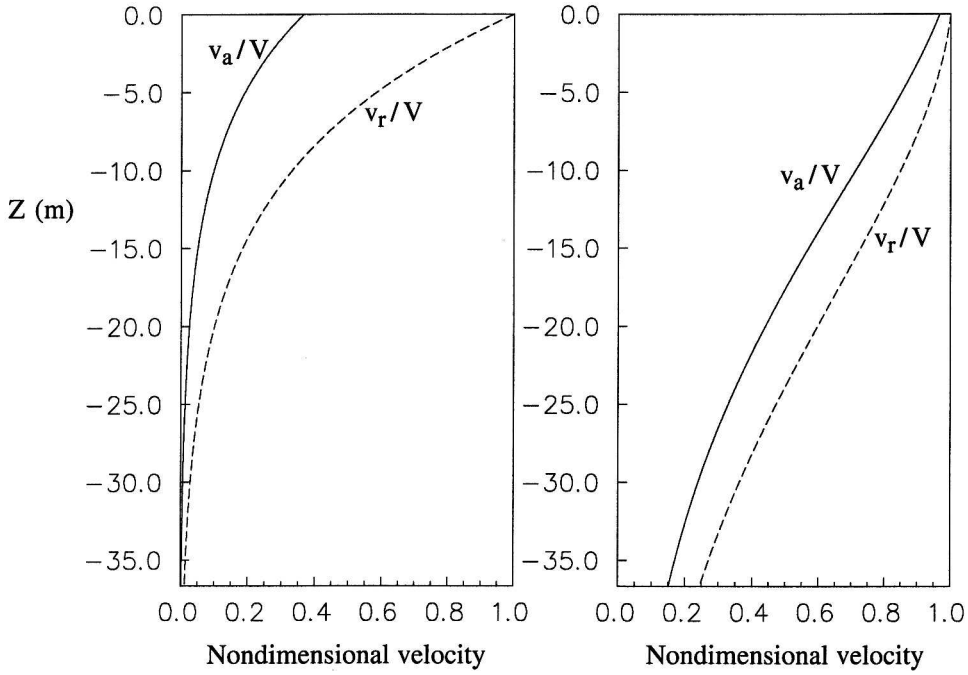

FIG. 2. Air and raindrop velocity profiles at (left) $T = 2$ min and (right) $T = 15$ min. Solid lines depict profiles of v_a/V. Dashed lines depict profiles of v_r/V.

for the first few minutes after the onset of the rain there is a substantial lag of the air velocity behind the rain velocity. However, during the last few minutes shown in Fig. 1 and continuing through later times (not shown), this lag is reduced to ~10%. Also, during the last few minutes shown in Fig. 2 and at later times (not shown), both v_a and v_r exhibit a slowly varying dependence on z, with the zone of maximum shear descending at a nearly constant rate of ~0.02 m s^{-1}. From (12) we see that if v_a were exactly equal to v_r, then v_a would not change with time. The descent speed of the shear zone is associated with this small but persistent lag.

Returning to the nondimensional description, $Z_f^*(t)$ is defined as the height of the maximum wind shear. Differentiating (23) with respect to Z^* (for $-T^* < Z^*$), and applying the recursion formula $dI_0(\eta)/d\eta = I_1(\eta)$, we get,

$$\frac{\partial^2 v^*}{\partial T^* \partial Z^*} = q_r(1-q_r)e^{-q_rT^*+(1-q_r)Z^*} \times I_0[2\sqrt{-q_rZ^*(T^*+Z^*)}] - q_re^{-q_rT^*+(1-q_r)Z^*}\frac{\sqrt{q_r}(T^*+2Z^*)}{\sqrt{-Z^*(T^*+Z^*)}} \times I_1[2\sqrt{-q_rZ^*(T^*+Z^*)}]. \quad (24)$$

Setting $\partial^2 v^*/\partial T^* \partial Z^* = 0$ at $Z^* = Z_f^*$ we find that Z_f^* must satisfy

$$(1-q_r)I_0[2\sqrt{-q_rZ_f^*(T^*+Z_f^*)}] = \frac{\sqrt{q_r}(T^*+2Z_f^*)}{\sqrt{-Z^*(T^*+Z_f^*)}} I_1[2\sqrt{-q_rZ_f^*(T^*+Z_f^*)}]. \quad (25)$$

Since $0 \le q_r < 1$ and the modified Bessel functions are positive for positive real arguments, we find that if Z_f^* exists then

$$T^* + 2Z_f^* > 0. \quad (26)$$

Attention is restricted to arguments $\eta \equiv 2\sqrt{-q_rZ_f^*(T^*+Z_f^*)}$ large enough to safely use the asymptotic approximations: $I_0(\eta) \sim I_1(\eta) \sim (2\pi\eta)^{-1/2} e^{\eta}$ [the approximated values of $I_0(\eta)$ and $I_1(\eta)$ are in good agreement with the tabulated values for $\eta \ge 4$ (the relative errors in the approximated values of I_0 and I_1 at $\eta = 4$ are within ~4% and ~12% of their respective tabulated values, and the errors decrease rapidly with increasing η). Applying these asymptotic formulas in (25), squaring both sides, and solving the resulting quadratic equation for Z_f^*, results in,

$$Z_f^* \approx -\frac{T^*}{2}\left[1 \pm \left(\frac{1-q_r}{1+q_r}\right)\right]. \quad (27)$$

In view of (26) we must choose the negative root in (27). It follows that $Z_f^* \sim -q_r T^*(1 + q_r)^{-1} \sim -q_r T^*$, and the descent speed of the shear zone is $C^* \equiv dZ_f^*/dT^* \sim -q_r$. In dimensional terms, the descent speed is the terminal velocity reduced by a factor of the rainwater mixing ratio,

$$C \approx q_r w_t. \tag{28}$$

Here, C is independent of time, and depends on the drag only implicitly, that is, through the terminal velocity.

To determine the range of times for which (28) is valid, apply $Z_f^* = -q_r T^*$ in the inequality $2\sqrt{-q_r Z_f^*(T^* + Z_f^*)} > 4$, and rearrange the result. We obtain $T^* > 2/[q_r(1 - q_r)] \sim 2/q_r$, or, in dimensional terms, $T > 2/(\lambda q_r)$.

Applying (28) with the restriction $T > 2/(\lambda q_r)$ to the heavy rain case considered in this section, we obtain a propagation speed $C \sim 0.023$ m s^{-1} for times $T > 530$ s. This estimate is consistent with the propagation speed from the full solution evident in Fig. 1.

4. Uniform shear flow

Guided by the behavior of the solution of the initial value problem, the evolution of uniform shear profiles for the air and raindrops is considered. Vertically propagating solutions of the form, $\upsilon_a = A\,(Z - CT) + F$, and $\upsilon_r = B(Z - CT) + E$ are sought , where A and B are constant shear parameters, and C is a constant propagation speed ($C < 0$ for descent). Substituting these forms in (11) and (12), we obtain $-BC + Bw_t = \lambda[(A - B)\,(Z - CT) + F - E]$ and $-CA = -q_r\,\lambda[(A - B)\,(Z - CT) + F - E]$, which can only be satisfied for $B = A$, $E = F - (CA/q_r\lambda)$, and $C = q_r w_t/(1 + q_r) \sim q\,w_t$. Thus the shear values are the same for both the air and raindrops, and the descent speed C is the same as in the initial value problem, namely Eq. (28). Omitting the parameter F (which is superfluous since it shifts the air and rain velocity profiles an equal amount), the solutions can be written as

$$v_a = A(Z - CT), \tag{29a}$$

$$v_r = A(Z - CT) - \frac{CA}{q_r\lambda}. \tag{29b}$$

The air and raindrop velocity profiles (29a) and (29b) are identical apart from an additive constant, $\Delta\upsilon \equiv \upsilon_r - \upsilon_a = -CA/(q_r\lambda)$. This velocity offset is well approximated by

$$\Delta\upsilon \approx -w_t A/\lambda. \tag{30}$$

Taking into account notational differences [and recalling that $\lambda = -g\,(1 - \rho_d/\rho_r)/w_t$] it can be shown that (30) is equivalent to the corresponding formula for the velocity offset in the case of one-way coupling, Eq. (10) of Khain and Pinsky (1995). Remarkably, provision for two-way coupling in uniform shear flow results in a slow descent of both air and rain velocity profiles, but leaves the velocity offset unchanged from its value in one-way coupling.

Also, the rain velocity profile can be brought into correspondence with the air velocity profile by shifting it upward, that is, $\upsilon_r(Z - \Delta Z, T) = \upsilon_a(Z, T)$, where $\Delta Z = -C/(q_r\lambda) \sim -w_t/\lambda$ (positive since $w_t < 0$). As discussed in section 3, $-w_t/\lambda$ (and thus ΔZ) is the vertical distance a drop falling at terminal velocity traverses in one horizontal relaxation time.

In view of (9), these height and velocity offsets can be rewritten as

$$\Delta Z \approx \frac{4}{3}\frac{\rho_r}{\rho_a}\frac{D}{C_D}, \quad \Delta\upsilon \approx A\Delta Z. \tag{31}$$

The height-offset ΔZ is independent of the wind shear. For the heavy rain example considered in section 3, $\Delta Z \sim 3.43$ m.

5. Periodic vertical shear

An analysis of the two-way drag interaction within a realistic model of turbulence (i.e., one representing a realistic energy cascade within a three-dimensional flow field) is beyond the scope of the present investigation. However, as a preliminary step toward such an analysis, the effect of the drag interaction on periodically varying shear profiles of various vertical wavenumbers is considered. For convenience, each wavenumber mode will be referred to as an eddy, but bear in mind that these eddies do not interact with each other (linear system) and are a drastic idealization of real-world turbulent structures.

This analysis of two-way particle interaction with eddies of various vertical wavenumbers parallels the one-way theory developed in Stackpole (1961) and Bohne (1982). Bohne analyzed particle response in the time domain (Lagrangian framework, following raindrop motion) and imposed a particle-relative air velocity in the form a temporal oscillation with specified frequency. In view of Taylor's frozen turbulence hypothesis, this assumed Lagrangian form was equivalent in the Eulerian viewpoint to a steady-state air velocity profile of specified vertical wavenumber. Particle response to single-wavenumber eddies could readily be extended to a population of eddies of various wavenumbers via the superposition principle for linear systems. In the present study, a vertical wavenumber is specified, but it is anticipated that the eddies may undergo a drag-induced propagation and temporal decay. Consider provisional (trial) solutions of the form

$$v_r = A(T)\sin[k(z - cT) + \delta], \tag{32a}$$

$$v_a = B(T)\sin[k(z - cT)], \tag{32b}$$

where A and B are the time-dependent amplitudes, c is the phase speed, k is the wavenumber, and δ is the phase shift between the air and rain velocity profiles. Without loss of generality, δ can be restricted to the range $\delta \in [0, \pi]$ (phase shifts beyond this range could be relocated within this range by redefining δ and A). Because of the linearity of (11) and (12) one can envision (32a) and (32b) as governing the kth wavenumber mode of a flow comprised of a collection of eddies of various wavenumbers superimposed on a background shear flow given by (29a) and (29b).

Substituting (32a) and (32b) into (11) and (12), expanding the resulting equations with the addition formulas for $\sin(\phi + \delta)$ and $\cos(\phi + \delta)$ [where $\phi \equiv k(z - ct)$], and collecting terms with common factors of $\sin\phi$ and $\cos\phi$, we obtain

$$\frac{dA}{dt}\cos\delta + ckA\sin\delta - kw_tA\sin\delta = \lambda(B - A\cos\delta) \tag{33}$$

$$\frac{dA}{dt}\sin\delta - ckA\cos\delta + kw_tA\cos\delta = -\lambda A\sin\delta, \tag{34}$$

$$\frac{dB}{dT} = -q_r\lambda(B - A\cos\delta), \tag{35}$$

$$B = -\frac{q_r\lambda\sin\delta}{ck}A. \tag{36}$$

In order for (32a) and (32b) to be legitimate solutions of (11) and (12), A, B, c, and δ must satisfy (33)–(36) or equations derived from them.

Applying (36) in (35) yields $dA/dT = -A(q_r\lambda + ck\cot\delta)$, which has the solution,

$$A(T) = A(0)e^{-(q_r\lambda + ck\cot\delta)T}. \tag{37}$$

As we will see, $q_r\lambda + ck\cot\delta > 0$, so (37) describes a temporal decay.

Applying (37) in (34), and rearranging, we obtain

$$\cot\delta = \frac{\lambda(1 - q_r)}{k(2c - w_t)}. \tag{38}$$

With δ considered in the range $\delta \in [0, \pi]$, only the principal value of $\cot^{-1}$ needs to be considered when obtaining δ from (38). Applying (36) and (37) in (33), yields a second relation for δ,

$$c\lambda(1 - q_r) - c^2k\cot\delta + kc(c - w_t)\tan\delta = -\frac{q_r\lambda^2}{k}\tan\delta. \tag{39}$$

Eliminating δ from between (38) and (39), we obtain a quartic equation for c:

$$(1 - q_r)^2c(w_t - c) = q_r(2c - w_t)^2 - \frac{k^2}{\lambda^2}c(w_t - c)(2c - w_t)^2. \tag{40}$$

As shown in appendix B, the solution of (40) is

$$c = \frac{w_t}{2} + \frac{1}{2\sqrt{2}}\sqrt{w_t^2 - \frac{\lambda^2}{k^2}(1 + q_r)^2 + \sqrt{\left[w_t^2 + \frac{\lambda^2}{k^2}(1 + q_r)^2\right]^2 - \frac{16q_r\lambda^2w_t^2}{k^2}}}. \tag{41}$$

Appendix B also shows that for $q_r \ll 1$, (41) is well approximated by

$$c \approx \frac{q_rw_t}{1 + k^2w_t^2/\lambda^2}. \tag{42}$$

Since $q_r \ll 1$ holds even in cases of extreme rainfall, the approximate solution (42) should be very accurate for meteorological purposes. Equation (42) shows that c is much less than w_t for all wavenumbers. The upper bound on the propagation speed is q_rw_t, and this maximum speed is approached for eddies of vanishing wavenumber, that is, in the limit of infinite wavelength. This upper bound is the same as the propagation speed of the uniform shear flow in section 4 and the asymptotic propagation speed in the initial value problem in section 3.

Since $c \ll w_t$, (38) is well approximated as $\cot\delta \sim -\lambda/(kw_t)$, and $\sin\delta$ is well approximated as

$$\sin\delta \approx \sqrt{\frac{1}{1 + \lambda^2/(k^2w_t^2)}} \tag{43}$$

(positive root since $\delta \in [0, \pi]$). Thus, for small eddies ($k \gg \lambda/w_t$), the air velocity lags the rain velocity by a quarter of a wavelength, $\delta \sim \pi/2$, while for large eddies

($k \ll \lambda/w_t$), the air velocity lags the rain velocity by only a slight amount, $\delta \sim k\,|w_t|/\lambda \ll 1$.

Applying (43) and (42) in (36), we obtain

$$B \approx \sqrt{1 + k^2 w_t^2/\lambda^2}\,A. \tag{44}$$

Taking into account notational differences [and again using $\lambda = -g(1 - \rho_a/\rho_r)/w_t$], it can be shown that (44) is equivalent to (10) of Stackpole (1961) and (8) of Bohne (1982). Thus, even though two-way coupling results in a temporal decay of the rain and air velocity amplitudes A and B, the ratio of these amplitudes is the same as in the case of one-way coupling.

Returning to (37), we see that the *e*-folding decay time scale is

$$T_e \equiv \frac{1}{q_r\lambda + ck\cot\delta}. \tag{45}$$

In view of (42) and the approximation $\cot\delta \sim -\lambda/(kw_t)$, (45) can be rewritten as

$$T_e \approx \frac{1}{q_r\lambda}\left(1 + \frac{\lambda^2}{k^2 w_t^2}\right) > 0. \tag{46}$$

Thus, the decay times T_e decrease inversely with increasing mixing ratio. For fixed mixing ratio, the decay times decrease with increasing wavenumber (decreasing wavelength $2\pi\,k^{-1}$), and approach the value $(q_r\lambda)^{-1}$ in the limit of vanishing wavelength. The decay times in this small-wavelength limit are given in Table 1 for a range of drop diameters and rainwater mixing ratios generally characteristic of moderate to heavy rainfall. The behavior of T_e as a function of wavelength for these parameters is depicted in Fig. 3. The decay times vary with drop diameter in an intriguing manner: at small wavelengths, the smallest decay times are found for the smaller drops, but at large wavelengths, the smallest decay times are found for the larger drops. For any fixed drop size, the curve of decay time versus wavelength tends to flatten as the mixing ratio increases. Accordingly, the scale sensitivity of the decay is reduced at the higher mixing ratios.

As mentioned above, this transient analysis is preliminary, and should be amended for flows characterized by a fully turbulent high Reynolds number energy cascade. Since eddy turnover times are generally smaller than the drag-decay times given by (46) (e.g., an eddy with a 50 m radius and a 5 m s^{-1} velocity scale would have a ~60 s turnover time compared with a drag-decay time of ~600 s), it is unlikely that the direct effect of turbulence on any specific wavenumber mode would be as great as indicated in this analysis. However, the effect of drag on a downscale energy cascade should be cumulative, and one may speculate that the greatest impact may still be seen at the higher wavenumbers.

Although a transient analysis of this problem is beyond the scope of this study, a simple qualitative analysis of the impact of drag on the energy transfer rate can be done for the stationary state. Restricting attention to wavenumbers small enough that dissipation is negligible ($k < k_1$ where k_1^{-1} is on the order of 10^{-2} m) but large enough that energy production is negligible ($k > k_0$ where k_0^{-1} is on the order of 10^2 m), the energy-spectrum balance equation (Pope 2000) with a drag parameterization is

$$\frac{\partial E}{\partial T} = -\frac{\partial F}{\partial k} - \frac{E}{T_e}. \tag{47}$$

Here E is the energy-spectrum function, F is the spectral energy transfer rate, and the drag has been parameterized as E/T_e [T_e given by (46)] so that in the absence of an energy transfer, the solution of (47) would be a temporally decaying energy-spectrum function with *e*-folding time T_e. We seek the downscale/upscale energy transfer ratio $F(k_1)/F(k_0)$ at times long enough after the onset of heavy rain that a stationary energy spectrum has been re-established, that is, when (47) has only drag and energy-transfer terms. In the absence of drag, F is constant across the inertial subrange [$F(k_1) = F(k_0) =$ dissipation rate ε] so $F(k_1)/F(k_0) = 1$. In the presence of drag, $F(k_1)$ can be obtained by integrating (47) from k_0 to k_1. Although it is not known how the energy-spectrum function is reduced in heavy rain, the Kolmogorov spectrum should be at least qualitatively valid. Applying $E = \alpha\varepsilon^{2/3}k^{-5/3}$ ($\alpha = 1.6$ is a universal constant) in $\int_{k_0}^{k_1}(E/T_e)\,dk$, introducing the variable $\xi(k) \equiv (w_t k/\lambda)^{2/3}$, and using Eq. (165.11) of Dwight (1961), we find

$$\begin{aligned} F(k_1) &= F(k_0) - \frac{3}{2}\,q_r\lambda^{1/3}\alpha\varepsilon^{2/3}w_t^{2/3}\int_{\xi(k_0)}^{\xi(k_1)}[\xi/(\xi^3+1)]\,d\xi, \\ &= F(k_0) - \frac{3}{2}\,q_r\lambda^{1/3}\alpha\varepsilon^{2/3}w_t^{2/3}\left[\frac{1}{6}\ln\frac{1-\xi+\xi^2}{(1+\xi)^2}\right. \\ &\quad \left. + \frac{1}{\sqrt{3}}\tan^{-1}\frac{2\xi-1}{\sqrt{3}}\right]_{\xi(k_0)}^{\xi(k_1)}. \end{aligned} \tag{48}$$

In heavy rain, ξ_1 is on the order of 10^2, and ξ_0 is on the order of 10^{-1}. In this case the error committed in (48) by replacing $\xi(k_1)$ by ∞ and $\xi(k_0)$ by 0, can be shown to be quite small (generally less than 10% for ε in the range $10^{-4} - 10^{-1}$ m^2 s^{-3}). Making these approximations in (48), normalizing the result by $F(k_0)$, and applying $F(k_0) = \varepsilon$ on the right-hand side, we obtain

$$\frac{F(k_1)}{F(k_0)} = 1 - \frac{\pi}{\sqrt{3}}\,q_r\lambda^{1/3}\alpha\varepsilon^{-1/3}w_t^{2/3}. \tag{49}$$

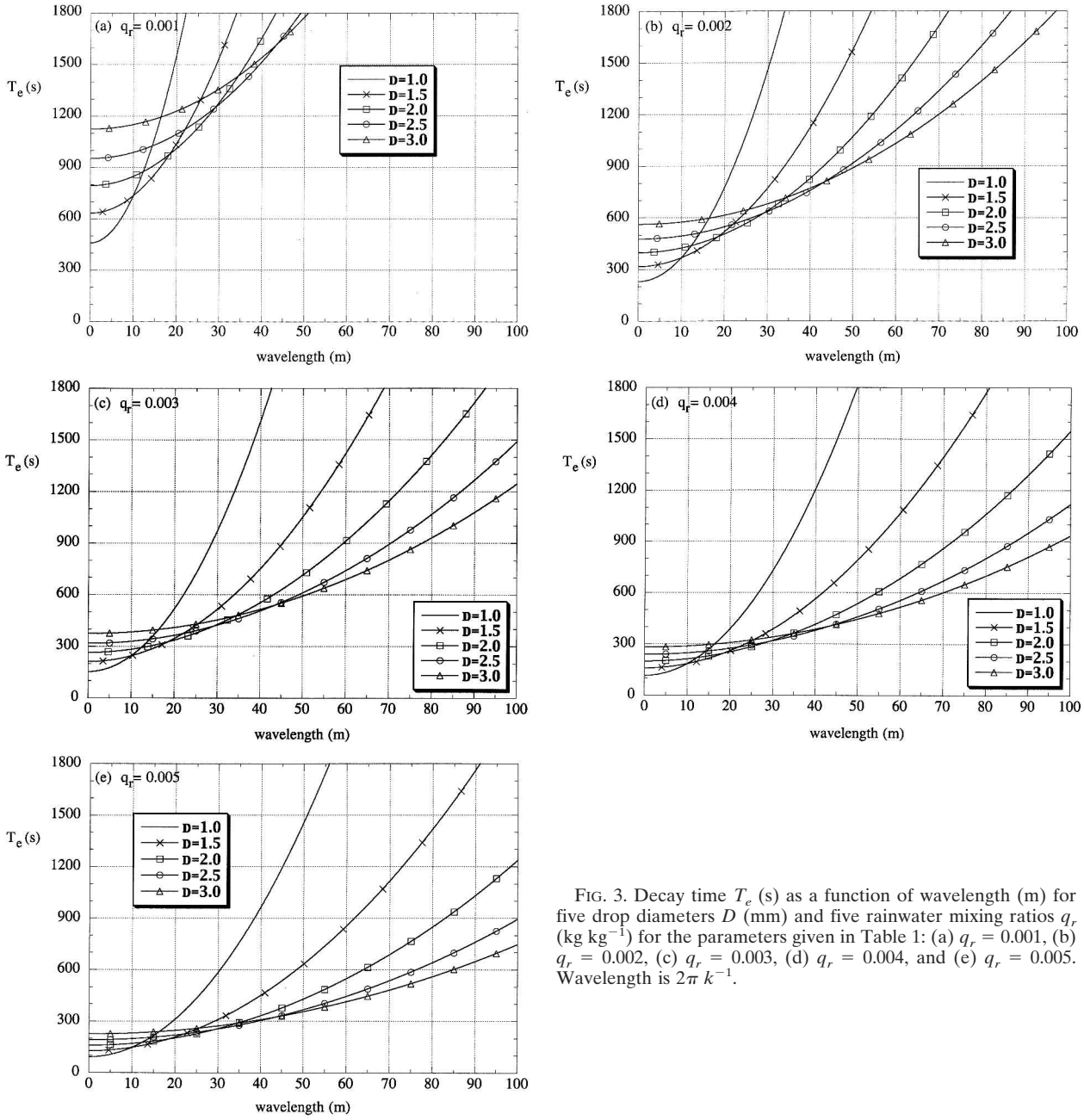

FIG. 3. Decay time T_e (s) as a function of wavelength (m) for five drop diameters D (mm) and five rainwater mixing ratios q_r (kg kg^{-1}) for the parameters given in Table 1: (a) $q_r = 0.001$, (b) $q_r = 0.002$, (c) $q_r = 0.003$, (d) $q_r = 0.004$, and (e) $q_r = 0.005$. Wavelength is $2\pi\, k^{-1}$.

Thus, the downscale reduction of the energy transfer rate becomes more pronounced at higher rainwater mixing ratios and lower dissipation rates. We calculate the energy transfer ratio (49) for the heavy rain parameters considered in section 3 ($q_r = 0.003$, $w_t = 7.7$ ms^{-1}, and $\lambda = 1.26$ s^{-1}), and several observed dissipation rates. Brewster and Zrnic (1986) report dissipation rates in the range $10^{-2} - 10^{-1}$ m^2 s^{-3} for a severe Oklahoma thunderstorm, which would correspond to heavy-rain energy transfer ratios of 0.83–0.92. Meischner et al. (2001) report dissipation rates in several strong and weak thunderstorm cells generally in the range $10^{-4} - 10^{-1}$ m^2 s^{-3}, which would yield energy transfer ratios of 0.21–0.92. Chapman and Browning (2001) report dissipation rates in precipitating frontal zones in the range $10^{-4} - 10^{-2}$ m^2 s^{-3} with a spatially averaged value of 10^{-3} m^2 s^{-3}, which would correspond to energy transfer ratios of 0.21–0.83, with an average value of 0.63. These values suggest that drag may be important in reducing the high-wavenumber energy transfer rates in thunderstorms and precipitating frontal zones in heavy rain conditions.

6. Summary

A simple theory was presented for two-way drag coupling between air and raindrops in moderate to heavy rainfall. The coupled equations of motion for the horizontal velocity components of the air and raindrops were solved analytically for the case of (i) initial step change in velocity, (ii) uniform shear profile, and (iii) periodically varying vertical shears of various wavenumbers. The solution of (i) indicated a decay of the initial velocity discontinuity followed, at later times, by a slow descent of the shear zone at a speed $C = q_r w_t$, where q_r is the rainwater mixing ratio, and w_t is the terminal velocity. In the case of uniform shear, both air and rain velocity profiles descended at the same speed $C = q_r w_t$ as in the later stages of the initial value problem (i). Formulas were obtained in the uniform shear case for the shift in velocity (or height) that would bring the air velocity profile into correspondence with the rain velocity profile. The velocity offset was found to be the same as in the case of one-way coupling (Khain and Pinsky 1995).

The analysis of periodically varying vertical shears may be considered a preliminary step toward a more realistic analysis of turbulent flows. The relation connecting the amplitudes of the air and rain velocities [Eq. (44)] was found to be the same as in the one-way coupling studies of Stackpole (1961) and Bohne (1982). However, unlike the one-way coupling studies, provision for two-way coupling leads to a smoothing of the velocity gradients (and a slow descent of the profiles). A key result is a formula [Eq. (46)] for the decay time as a function of mixing ratio, drag parameter, and wavenumber. The decay times decrease with decreasing wavelength, and approach a value equal to the reciprocal of the product of the rainwater mixing ratio and a drag parameter. For the smallest-scale structures, the decay times are on the order of a few minutes for moderate to heavy rainfall. However, since realistic turbulent eddies lie within an energy cascade, we should anticipate that the inexorable churning of larger eddies into smaller eddies would partially mitigate the temporal decay forced by the drag interaction. High-resolution numerical modeling may be the most appropriate tool to study this more realistic problem.

Acknowledgments. The author is grateful to Evgeni Fedorovich, Yefim Kogan, Dick Doviak, Edwin Kessler, and Mike Biggerstaff for discussions on various aspects of this work. Contour plots were prepared with ZXPLOT graphics software developed by Ming Xue. Mark Laufersweiller provided computer assistance. The author was supported in part by the Engineering Research Centers Program of the National Science Foundation (NSF) under NSF Award Number 0313747, by NSF ATM-333872 and by NSF ATM-0129892. Any opinions, findings, conclusions, or recommendations expressed in this study are those of the author and do not necessarily reflect those of the National Science Foundation.

APPENDIX A

Solution of the Initial Value Problem

The initial value problem (13) and (14) is solved for a step change in velocity profile with the method of Laplace transforms (e.g., Doetsch 1961; and other standard references). Multiplying (13) by e^{-sT} and integrating over time from $T = 0$ to $T = \infty$, we obtain a first-order ordinary differential equation for $\hat{v} = L(v_a) = \int_0^\infty v_a e^{-sT}\, dT$, the Laplace transform of v_a,

$$w_t(s + \lambda q_r)\frac{d\hat{v}}{dZ} + s[s + \lambda(q_r + 1)]\hat{v} - \left\{ w_t \frac{\partial v_a}{\partial Z} + \frac{\partial v_a}{\partial T} + [s + \lambda(q_r + 1)]v_a \right\}\Bigg|_{T=0} = 0. \tag{A1}$$

Applying the initial data (14) and $\partial v_a(Z, 0)/\partial T = 0$ [the latter obtained by applying (14) in (12)] in (A1) we obtain,

$$w_t(s + \lambda q_r)\frac{d\hat{v}}{dZ} + s[s + \lambda(q_r + 1)]\hat{v} - V\{w_t\delta(Z) + [s + \lambda(q_r + 1)]H(Z)\} = 0, \tag{A2}$$

where $\delta(Z) = dH/dZ$ is the Dirac delta function.

For $Z > 0$, the solution of (A2) is $\hat{v} = V/s$, and the inverse transform yields the expected result, $v_a(Z, t) = V$. For $Z < 0$ the solution of (A2) is readily found to be,

$$\hat{v} = \alpha \exp\left\{ -\frac{s[s + \lambda(q_r + 1)]}{s + \lambda q_r} Z/w_t \right\}, \tag{A3}$$

To evaluate α, integrate (A2) with respect to Z from $-\varepsilon$ to ε (where $\varepsilon > 0$). In the limit $\varepsilon \to 0$ we obtain the jump condition,

$$\hat{v}(0^+) - \hat{v}(0^-) = \frac{V}{s + \lambda q_r}. \tag{A4}$$

Since $\hat{v}(0^-) = \alpha$ and $v(0^+) = V/s$, it follows from (A4) that, $\alpha = V\lambda q_r/[s\,(s + \lambda q_r)]$. With α thus determined, v_a is obtained as the inverse transform of (A3),

$$v_a = L^{-1}\left\langle \frac{V\lambda q_r}{s(s + \lambda q_r)} \exp\left\{ -\frac{s[s + \lambda(q_r + 1)]}{s + \lambda q_r} Z/w_t \right\} \right\rangle. \tag{A5}$$

Rewriting the curly bracketed term in (A5) as,

$$-\frac{s[s+\lambda(q_r+1)]}{s+\lambda q_r}Z/w_t = -sZ/w_t - \lambda Z/w_t + \frac{\lambda^2 q_r}{s+\lambda q_r}Z/w_t, \quad \text{(A6)}$$

(A5) becomes

$$v_a = V\lambda q_r e^{-\lambda Z/w_t} \times L^{-1}\left[\frac{e^{-sZ/w_t}}{s}\frac{1}{s+\lambda q_r}\exp\left(\frac{\lambda^2 q_r}{s+\lambda q_r}Z/w_t\right)\right]. \quad \text{(A7)}$$

Applying the convolution theorem to (A7), we obtain

$$v_a = V\lambda q_r e^{-\lambda Z/w_t}\int_0^T F(\tau)G(T-\tau)\,d\tau, \quad \text{(A8)}$$

where

$$F(T) = L^{-1}\left(\frac{e^{-sZ/w_t}}{s}\right),$$

$$G(T) = L^{-1}\left[\frac{1}{s+\lambda q_r}\exp\left(\frac{\lambda^2 q_r}{s+\lambda q_r}Z/w_t\right)\right]. \quad \text{(A9)}$$

It can readily be shown that $F(T) = H(T - Z/w_t)$. To evaluate $G(T)$ we use the Bromwich integral,

$$G(T) = \frac{1}{2\pi i}\int_{c-i_\infty}^{c+i_\infty}\frac{e^{sT}}{s+\lambda q_r}\exp\left(\frac{\lambda^2 q_r}{s+\lambda q_r}Z/w_t\right)ds, \quad \text{(A10)}$$

where c is any real number large enough that all singularities of $L(G)$ lie in the complex half-plane to the left of c. Changing variables to $\sigma = s + \lambda q_r$, (A10) becomes

$$G(T) = \frac{e^{-\lambda q_r T}}{2\pi i}\int_{c+\lambda q_r-i_\infty}^{c+\lambda q_r+i_\infty}\frac{e^{\sigma T}}{\sigma}\exp\left(\frac{\lambda^2 q_r}{\sigma}Z/w_t\right)d\sigma. \quad \text{(A11)}$$

We extend the integral in (A11) to the closed contour consisting of the original path of integration (line parallel to the imaginary axis), and a semicircle of infinite radius affixed to (and to the left of) this path (Fig. A1). This closed contour encloses one singularity, an essential singularity at $\sigma = 0$. Since the integral vanishes on the semicircle, the integral in (A11) along the original path is equal to the integral over the closed contour, and the residue theorem yields

$$G(T) = e^{-\lambda q_r T} \times \operatorname*{Res}_{\sigma=0}\left[\frac{e^{\sigma T}}{\sigma}\exp\left(\frac{\lambda^2 q_r}{\sigma}Z/w_t\right)\right]. \quad \text{(A12)}$$

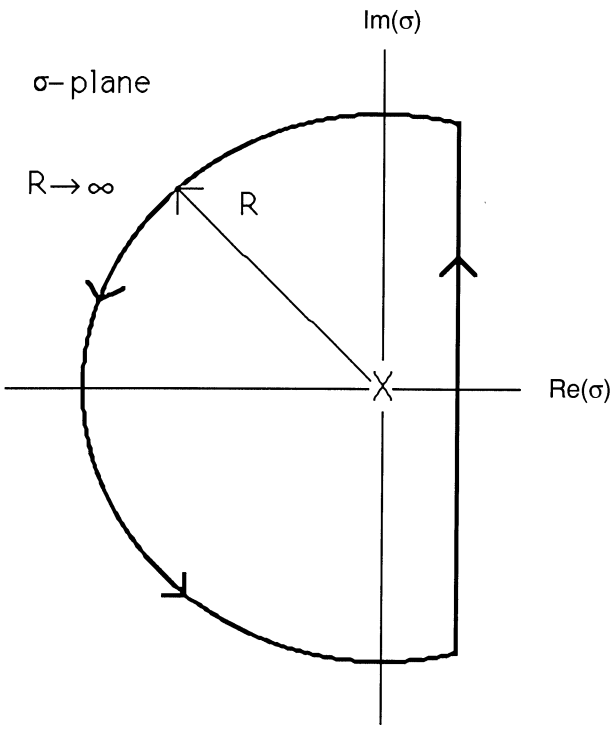

FIG. A1. Closed contour in complex σ plane used to evaluate the Laplace inversion integral (A11). The contour encloses an essential singularity (denoted by X) at $\sigma = 0$.

Expanding $e^{\sigma T}$ and $\exp[\lambda^2 q_r Z/(w_t\sigma)]$ in Laurent series about the singularity, (A12) becomes

$$G(T) = e^{-\lambda q_r T} \times \operatorname{Res}_{\sigma=0}\left[\sum_{m=0}^{\infty}\sum_{n=0}^{\infty}\sigma^{m-n-1}\frac{T^m}{m!n!}(\lambda^2 q_r Z/w_t)^n\right]. \quad \text{(A13)}$$

The residue (coefficient of $1/\sigma$) is the sum of terms for which $m = n$, and can be put in the form

$$\sum_{n=0}^{\infty}\frac{T^n}{n!^2}(\lambda^2 q_r Z/w_t)^n = \sum_{n=0}^{\infty}\frac{(2\lambda\sqrt{q_r TZ/w_t})^{2n}}{n!^2 2^{2n}} = I_0(2\lambda\sqrt{q_r TZ/w_t}), \quad \text{(A14)}$$

where I_0 is the modified Bessel function of the first kind of order zero (Abramowitz and Stegun 1964).

Collecting results, (A8) becomes

$$v_a = V\lambda q_r e^{-\lambda Z/w_t}\int_0^T H(\tau - Z/w_t) \times e^{-\lambda q_r(T-\tau)}I_0(2\lambda\sqrt{q_r(T-\tau)Z/w_t})\,d\tau. \quad \text{(A15)}$$

Applying the definition of H in (A15), and recalling that $v_a(Z, t) = V$ for $Z > 0$, the full solution for v_a can be written as

$$v_a = \begin{cases} V, & Z > 0. \\ Ve^{-\lambda Z/w_t} \int_0^{\lambda q_r (T - Z/w_t)} e^{-u} I_0(2\sqrt{\lambda Z u / w_t})\, du, & -T < -Z/w_t < 0, \\ 0, & -Z/w_t < -T < 0. \end{cases} \quad \text{(A16)}$$

APPENDIX B

Solution of the Quartic Equation for *c*

As shown in section 5, the phase speed c for vertical propagation of eddies of wavenumber k in the presence of rainfall satisfies (40), a quartic equation. Fortunately, this quartic equation can be rewritten as a quadratic equation for a quadratic function of c, namely,

$$G^2 + G\left[w_t^2 + \frac{\lambda^2}{k^2}(1 + q_r)^2 \right] + 4q_r w_t^2 \frac{\lambda^2}{k^2} = 0, \quad \text{(B1)}$$

where

$$G \equiv 4c(c - w_t). \quad \text{(B2)}$$

Solving (B1) for G, we obtain

$$G = -\frac{1}{2}\left[w_t^2 + \frac{\lambda^2}{k^2}(1 + q_r)^2 \right] + \frac{1}{2}\sqrt{\left[w_t^2 + \frac{\lambda^2}{k^2}(1 + q_r)^2 \right]^2 - \frac{16 q_r \lambda^2 w_t^2}{k^2}}, \quad \text{(B3)}$$

where we have chosen the positive branch of the solution (it can be shown that the negative branch would yield a complex value for c). Solving (B2) for c and making use of (B3), we obtain

$$c = \frac{w_t}{2} + \frac{1}{2\sqrt{2}}\sqrt{w_t^2 - \frac{\lambda^2}{k^2}(1 + q_r)^2 + \sqrt{\left[w_t^2 + \frac{\lambda^2}{k^2}(1 + q_r)^2 \right]^2 - \frac{16 q_r \lambda^2 w_t^2}{k^2}}} \quad \text{(B4)},$$

where we have again chosen the positive branch of the solution [the negative branch does yield a real value for c ($c \approx w_t$), but such a solution corresponds to $B \approx A/q_r$, a nonmeteorological scenario in which the rain velocity is several orders of magnitude greater than the air velocity].

A useful approximation to (B4) can be obtained for $q_r \ll 1$. First, rewrite (B4) as,

$$c = \frac{w_t}{2} + \frac{|w_t|}{2\sqrt{2}} \times \sqrt{(1 - x) + (1 + x)\sqrt{1 - \frac{16 q_r}{(1 + q_r)^2}\frac{x}{(1 + x)^2}}}, \quad \text{(B5)}$$

where

$$x \equiv \frac{\lambda^2}{k^2 w_t^2}(1 + q_r)^2. \quad \text{(B6)}$$

Since the maximum value of $x/(1 + x)^2$ is 1/4 (obtained at $x = 1$) and since $q_r \ll 1$, we see that

$$\frac{16 q_r}{(1 + q_r)^2}\frac{x}{(1 + x)^2} < \frac{4 q_r}{(1 + q_r)^2} < 4q_r \ll 1. \quad \text{(B7)}$$

Thus, we may safely impose the binomial approximation to the innermost radical in (B5). After some rearrangement, we obtain

$$c \approx \frac{w_t}{2} + \frac{|w_t|}{2}\sqrt{1 - \frac{4 q_r}{(1 + q_r)^2}\frac{x}{1 + x}}. \quad \text{(B8)}$$

Since the maximum value of $x/(1 + x)$ is 1 (approached as $x \to \infty$), we see that

$$\frac{4 q_r}{(1 + q_r)^2}\frac{x}{1 + x} < \frac{4 q_r}{(1 + q_r)^2} \ll 1. \quad \text{(B9)}$$

Accordingly, we can impose the binomial approximation in (B8), obtaining

$$c \approx \frac{w_t}{2} + \frac{|w_t|}{2}\left[1 - \frac{2 q_r}{(1 + q_r)^2}\frac{x}{1 + x} \right]. \quad \text{(B10)}$$

Substituting in (B6) for x, using the fact that w_t is negative, and applying the approximation $(1 + q_r)^2 \sim 1$, (B10) becomes

$$c \approx \frac{q_r w_t}{1 + k^2 w_t^2/\lambda^2}. \quad \text{(B11)}$$

REFERENCES

Abramowitz, M., and I. A. Stegun, Eds., 1964: *Handbook of Mathematical Functions with Formulas, Graphs, and Mathematical Tables*. National Bureau of Standards, 1046 pp.

Beard, K. V., 1976: Terminal velocity and shape of cloud and precipitation drops aloft. *J. Atmos. Sci.,* **33,** 851–864.

Bohne, A. R., 1982: Radar detection of turbulence in precipitation environments. *J. Atmos. Sci.,* **39,** 1819–1837.

Brewster, K. A., and D. S. Zrnic, 1986: Comparison of eddy dissipation rates from spatial spectra of Doppler velocities and

Doppler spectrum widths. *J. Atmos. Oceanic Technol.,* **3,** 440–452.
Caldwell, D. R., and W. P. Elliott, 1972: The effect of rainfall on the wind in the surface layer. *Bound.-Layer Meteor.,* **3,** 146–151.
Chapman, D., and K. A. Browning, 2001: Measurements of dissipation rate in frontal zones. *Quart. J. Roy. Meteor. Soc.,* **127,** 1939–1959.
Doetsch, G., 1961: *Guide to the Applications of Laplace Transforms*. Van Nostrand, 255 pp.
Dwight, H. B., 1961: *Tables of Integrals and Other Mathematical Data*. 4th ed. Macmillan, 336 pp.
Khain, A. P., and M. B. Pinsky, 1995: Drop inertia and its contribution to turbulent coalescence in convective clouds. Part I: Drop fall in the flow with random horizontal velocity. *J. Atmos. Sci.,* **52,** 196–206.
Kundu, P. K., and I. M. Cohen, 2002: *Fluid Mechanics*. 2d ed. Academic Press, 730 pp.
Meischner, P., R. Baumann, H. Höller, and T. Jank, 2001: Eddy dissipation rates in thunderstorms estimated by Doppler radar in relation to aircraft in situ measurements. *J. Atmos. Oceanic Technol.,* **18,** 1609–1627.
Pinsky, M., and A. Khain, 1997: Turbulence effects on droplet growth and size distribution in clouds—A review. *J. Aerosol Sci.,* **28,** 1177–1214.
Pope, S. B., 2000: *Turbulent Flows*. Cambridge University Press, 771 pp.
Shaw, R. A., 2003: Particle–turbulence interactions in atmospheric clouds. *Annu. Rev. Fluid Mech.,* **35,** 183–227.
Stackpole, J. D., 1961: The effectiveness of raindrops as turbulence sensors. *Proc. Ninth Weather Radar Conf.*, Kansas City, MO, Amer. Meteor. Soc., 212–217.
Stout, J. E., Y.-L. Lin, and S. P. S. Arya, 1993: A theoretical investigation of the effects of sinusoidal topography on particle deposition. *J. Atmos. Sci.,* **50,** 2533–2541.
——, S. P. Arya, and E. L. Genikhovich, 1995: The effect of nonlinear drag on the motion and settling velocity of heavy particles. *J. Atmos. Sci.,* **52,** 3836–3848.
Vaillancourt, P. A., and M. K. Yau, 2000: Review of particle–turbulence interactions and consequences for cloud physics. *Bull. Amer. Meteor. Soc.,* **81,** 285–298.
White, F. M., 1991: *Viscous Fluid Flow*. 2d ed. McGraw-Hill, 614 pp.